IPPI

Polyolefins Journal Vol. 10, No. 2 (2023)
DOI: 10.22063/POJ.2023.3316.1254

ORIGINAL PAPER

Exploring the possibility of chemisorption of ethylene on graphene with and without defects

Parisa Alamdari[1], Farhad Sharif[1,*], Saeedeh Mazinani[2]

[1]Department of Polymer Engineering and Color Technology, Amirkabir University of Technology, Tehran, Iran
[2]New Technologies Research Center (NTRC), Amirkabir University of Technology, Tehran, Iran

Received: 26 January 2023, Accepted: 16 April 2023

ABSTRACT

The effect of structural defects on graphene interaction with other molecules is of high interest. In this study, the interaction of ethylene molecules with pristine graphene (PG) and defective graphenes including single (SVG) and double (DVG) vacancies, were investigated using dispersion-corrected periodic density functional theory (DFT). We used various pairs of pseudopotentials and dispersion-corrected methods to calculate the exchange-correlation energies and long-range energies, respectively. We conducted the calculations in the ethylene-graphene equilibrium distance where vdW interaction as a long-range interaction was dominant. Both adsorption and deformation energies were calculated to examine the possibility of ethylene chemisorption. It was found that there is a critical distance from the graphene surface, where the nature of adsorption of adsorbate molecule changes from physisorption to the possible chemisorption depending on the energetical costly distortion induced in adsorbate molecule. In the case of ethylene adsorption on the graphene structures studied here, the mentioned critical distances follow the order SVG < DVG < PG. However, in the range of vdW domination and in comparison with PG, ethylene interacts more with SVG due to the presence of a dangling bond and interacts less with DVG due to the presence of a hole. Furthermore, the interactions of ethylene with reconstructed trivacancy were studied. Moreover, all possible orientations for ethylene adsorption on graphene structures were considered and energetically compared. All calculations were done on fully optimized reconstructed geometries of vacancies with structural characteristics, i.e., reconstruction length and formation energies comparable to those reported in the literature. **Polyolefins J (2023) 10: 101-115**

Keywords: Carbon dimer; carbon vacancy; DFT; adsorption; active site.

INTRODUCTION

Since the advent of graphene in 2004 [1], this material has attracted much attention from researchers, academics, and industries to investigate absorption-based phenomena due to its high surface area, tunable structure, and potential stable precursors. [2-6]. The growing effort to rationally tune the structure and composition of graphene has made it an amazing platform for advanced material design and has led to vast development of graphene-based materials with multiple roles in chemical reactions. Since adsorption lies at the heart of chemical reactions, it is highly important to understand how graphene and its derivatives interact with other molecules in its vicinity.

Ethylene, as the most widely produced organic compound in the world has been used in manufacturing of numerous products [7]. Therefore, ethylene is one of the molecules which the study of its interaction with graphene

---

*Corresponding Author - E-mail: sharif@aut.ac.ir

is significantly important. From the literature, graphene derivatives have been evaluated in some ethylene participating reactions as catalyst [8-11] and in some other cases as catalyst support [9, 12, 13]. However, in order to improve the performance of graphene in these reactions, enough knowledge on the nature of active sites and the effect of graphene structural characteristics on its properties is necessary [14].

In the absence of metals, graphene has been used as highly active catalyst for selective hydrogenation of acetylene in the presence of large excess ethylene, in 2014 [8]. Selective acetylene hydrogenation as an industrially important reaction still requiring metals as catalysts. Due to the permanent poisoning effect of acetylene on ethylene polymerization catalysts, it is essential to omit even small amount of acetylene in the ethylene feed. Recently, it has been proved that frustrated Lewis pairs in which, steric hindrance could preclude Lewis adduct formation, could be used to split hydrogen-hydrogen bond in H_2 [15]. However, the hydrogen dissociation by intrinsic defects of graphene has been introduced as the source of graphene catalytic activity in acetylene hydrogenation, and the exact mechanism of this catalytic activity is still unclear [16].

In the case of ethylene polymerization, although graphene widely has been studied as either catalyst support [17-21] or filler [22-24] to incorporating special properties in polymeric matrix, there is no evidence in literature on intrinsic catalytic activity of graphene in this industrially important reaction. However, even in these cases, the interaction of ethylene with graphene as catalyst support or filler is important.

Due to the lack of complete knowledge on the mechanism of reactions involving carbocatalysts, even by inspiration from similar organic reactions, there will be numerous possibilities which must be evaluated to find the most reasonable reaction path. Furthermore, synergy or antagonism between unavoidable coexistent sites should be considered. In such a complex system, theoretical calculations based on density functional theory (DFT) are of significant importance in providing a more precise view of what is happening during the reaction. Since structural defects formation is unavoidable in mass production of graphene, the study of the interaction of ethylene molecule with graphene defects as a part of complex interactions during the catalytic reactions is important.

In 2020, Li and co-worker using the DFT method studied the interaction of small hydrocarbon molecules, including ethylene, with graphene to explain the growth mechanism of pyrocarbon through chemical vapor infiltration. This study indicated weak ethylene physisorption on pristine graphene. Furthermore, they revealed that the introduction of vacancy defect does not significantly affect the adsorption mechanism of ethylene [25]. Considering previous reports in literature on the healing of double carbon vacancy on graphene by ethylene adsorption [26], the extremely high reactivity of under-coordinated carbon atom at the edge of single carbon vacancy and the reports on its ability to break strong H-H bond of hydrogen molecule [16] it is essential to review the interaction of ethylene with pristine and defective graphene more precisely to shed light on the nature of its adsorption. On the other hand, it is really challenging to predict the nature and strength of small molecules' interaction with graphene especially when non-covalent long-range interactions exist. In order to distinguish between physisorption and chemisorption of small organic molecules on graphene, it is common to use adsorption energy. However, according to Lokalj [27] report, the adsorption energy is not a reliable criterion to this goal. Considering chemical bond formation as a more reliable characteristic for the chemisorption, the length and strength of the bonds between the small molecule and the surface better represent physical or chemical nature of the adsorption. Moreover, sizeable geometrical distortion during chemisorption is energetically costly. In addition to the geometrical characteristics of the studied system, the calculation method of exchange-correlation energy and long-range energy also affect the amount of adsorption energy.

This study aims to explore the nature of ethylene adsorption on graphene using the dispersion corrected periodic DFT method. Moreover, the influence of intrinsic structural defects on this interaction and all possible orientations for the ethylene adsorption on graphene structures were systemically investigated and compared. In this study for the first time we used various pairs of pseudopotentials and dispersion-corrected methods for the calculation of the exchange-correlation and long-range energies to emphasize the insufficiency of adsorption energy for describing the type of ethylene adsorption on graphene with and without structural defects. Furthermore, we show that in geometry optimization calculations, there is a critical distance between the adsorbate and the surface where the nature of adsorption changes from physisorption to chemisorption. This critical distance can be considered as a criterion to show either physisorption or chemisorption is more prone. The theoretical prediction of the nature of small molecules adsorption on graphene provides useful information on the potential applications of the adsorption phenomena.

EXPERIMENTAL

Computation method

All periodic DFT calculations were performed using the plane-wave self-field consistent Quantum Espresso package [28,29]. The plane-wave expansion of the wave functions is set to a kinetic energy cutoff of 400 eV. The k-points grid employed is set to 5×5×1 with the k-points automatically generated using the Monkhorst-Pack grid [30]. In order to achieve accurate electronic convergence, a Gaussian smearing of 0.01 Ry was applied. A 4×4×1 super-cell of graphene consisting of 32 carbon atoms was considered as the model. The distance between two adjacent graphene layers was kept at 20 Å to minimize the interactions between them. For structure relaxation, the atomic positions were fully optimized until the maximum force on each atom was less than 10^{-4} eV $Å^{-1}$, and the convergence criteria for energy was set to 10^{-6} eV. The adsorption energy was defined using the energy of graphene-based material GS, (E_{GS}), the energy of ethylene (E_{Eth}) and the energy of stable structure with the hydrocarbon adsorbed on GS ($E_{GS+(Eth)}$) as follows:

$$E_{ads} = E_{(GS+Eth)} - E_{GS} - E_{Eth} \quad (1)$$

Essences of using dispersion corrected DFT method

Since the adsorption of ethylene on the surface of graphene-based structures (GS) has strong contributions from van der Waals interactions (i.e., dispersion forces), it is essential to use dispersion correction for more accurate prediction of its adsorption energy on GS. For being more confident in this matter, the equilibrium distance between ethylene and PG, SVG and DVG was calculated with and without considering dispersion correction in DFT calculations. Here, the equilibrium distance refers to the ethylene distance from graphene plane, at which the total energy of system is minimum in the range of physisorption. In these calculations, the distance between ethylene and graphene plane was scanned using PBESOL pseudopotential and Grimme-2 method for van der Waals (vdW) correction. Moreover, the distances were selected in the range that vdW interactions as long-range interactions were dominant. Indeed, the ethylene distance from the surface of graphene plane was high enough to be sure that the adsorption includes no chemical bonding and is in the range of physisorption.

In all cases, not only the equilibrium distance shifts to lower value using dispersion correction, but also the total energy of the system decreases. The ethylene equilibrium distance to PG, SVG and DVG decreased from 3.3 to 2.7 Å, from 3.5 to 2.7 Å and from 3 to 2.7 Å, respectively, by implementing vdW correction. Therefore, it is essential to include vdW implemented DFT calculations for exploring ethylene interaction with PG, SVG and DVG structures. Moreover, the amount of shift in the equilibrium distance due to the vdW interaction is the highest in the case of SVG and is the lowest in the case of DVG. This emphasizes on stronger vdW interaction between ethylene and SVG and weaker vdW interaction between ethylene and DVG in comparison with PG, which may be attributed to the presence of a dangling bond in SVG and a hole in DVG.

Pseudopotential (PP) and vdW correction method

There are two general states for adsorption of ethylene on graphene: physisorption and chemisorption. In the case of chemisorption, the total energy of system is minimum and the length of all bonds should be in the equilibrium ranges. In the case of physisorption, in addition to the bonds' length, the orientation of molecule with respect to the surface and the distance between the molecule and surface should be in the equilibrium range to be sure about minimization of the system energy. To find this equilibrium distance, it is usual to scan the distance between molecule and surface using single point calculations. In this study, these initial calculations were conducted using PBESOL-D2.

Then, to study how adsorption energy is affected by pseudopotential and vdW correction method, we conducted some geometry optimizations by considering the previous equilibrium distances as estimation of initial distances for full optimizations. During geometry optimizations, the distance between the adsorbate and graphene surface approaches the equilibrium value. The results of these calculations have been illustrated in Figure 1. The adsorption energies of ethylene on GS were calculated using the equation of adsorption, as mentioned before:

Generally, physisorption is characterized by weak bonding and larger bond lengths (> 1.5 Å). Similar to the previous section, the calculations here were conducted in the range of physisorption, in which vdW interaction is more dominant. Therefore, no chemical bond was observed between ethylene and GS. In the case of SVG and DVG, the graphene structure was reconstructed due to the ethylene interaction. For almost all PP/vdW selections and in comparison with PG, ethylene interacts more with SVG and interacts less with DVG due to the presence of a dangling bond in SVG and a larger hole in DVG. Moreover, in comparison with ultra-soft PPs, norm-conserving PPs causes larger differences in ethylene adsorption energies on GS. On the other hand, the dispersion correction using Grimme-3 method causes more accurate ethylene adsorption energies than Grimme-2 method since contrary to Grimme-2, Grimme-3 is flexible and system dependent. Finally, the use of PBESOL-nc/Grimme-3 appears to reasonably predict the ethylene adsorption energy on GS. Therefore, the generalized gradient approximation (GGA) with the Perdew, Burke and Enzerhof (PBE) functional modified for solids was employed to calculate the exchange correlation energies of the different structures [31, 32] and to consider the effect of van der Waals (vdW) forces on the interaction of ethylene and graphene-based structures, and the long-range-dispersion-corrected Grimme D3 method was taken into account [33].

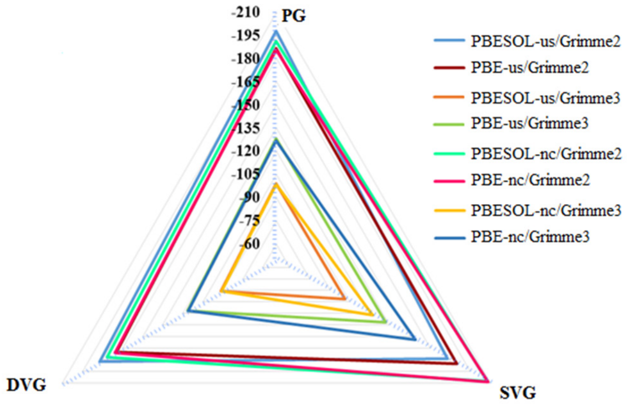

Figure 1. Ethylene adsorption energy on PG, SVG and DVG from calculations using different PP/vdW pairs.

RESULTS AND DISCUSSION

Reconstruction of defective graphene structures

The ideal geometry of studied GS has been represented in Figure 2. After full optimization, the SVG and DVG reconstruct themselves to more stable geometries with minimum number of under-coordinated carbenes through forming new semi-bonds. The new distance between nonbonding carbons in reconstructed SVG and DVG is 2.07 Å and 1.79 Å, respectively, in good agreement with literature [34] (see Table 1). Therefore, SVG should be more reactive than DVG due to less stabilization effect of two under-coordinated carbon atoms, moreover, the presence of one dangling bond. In the case of SVG, reconstruction slightly bends the plane of graphene and guides the SVG substrate to a less energetically unstable state by the value of 28.5 kJ mol^{-1}. This reconstruction in SVG is Jahn-Teller distortion, and nonlinear atomic arrangements having a degenerate electronic ground state undergo a geometric distortion to remove the degeneracy and thus lower the total energy of the system. The reconstructed DVG is more stable than DVG by the value of 189 kJ mol^{-1}.

Moreover, as shown in Figure 2, introducing carbon vacancies into the inert pristine graphene causes charge density localization, which is beneficial for more reactivity of defective graphene structures.

For the vacancies without an odd number of carbon atoms, at least one dangling bond persists, whereas for structures missing an even number of atoms more stable structures lacking dangling bonds are possible. In the case of multi-vacancies with an even number of missing atoms, the formation of lines of two or three DVG vacancies is observed in the graphene membrane under electron irradiation in HRTEM. In such pairs or lines, adjacent di-vacancies have a common pentagon

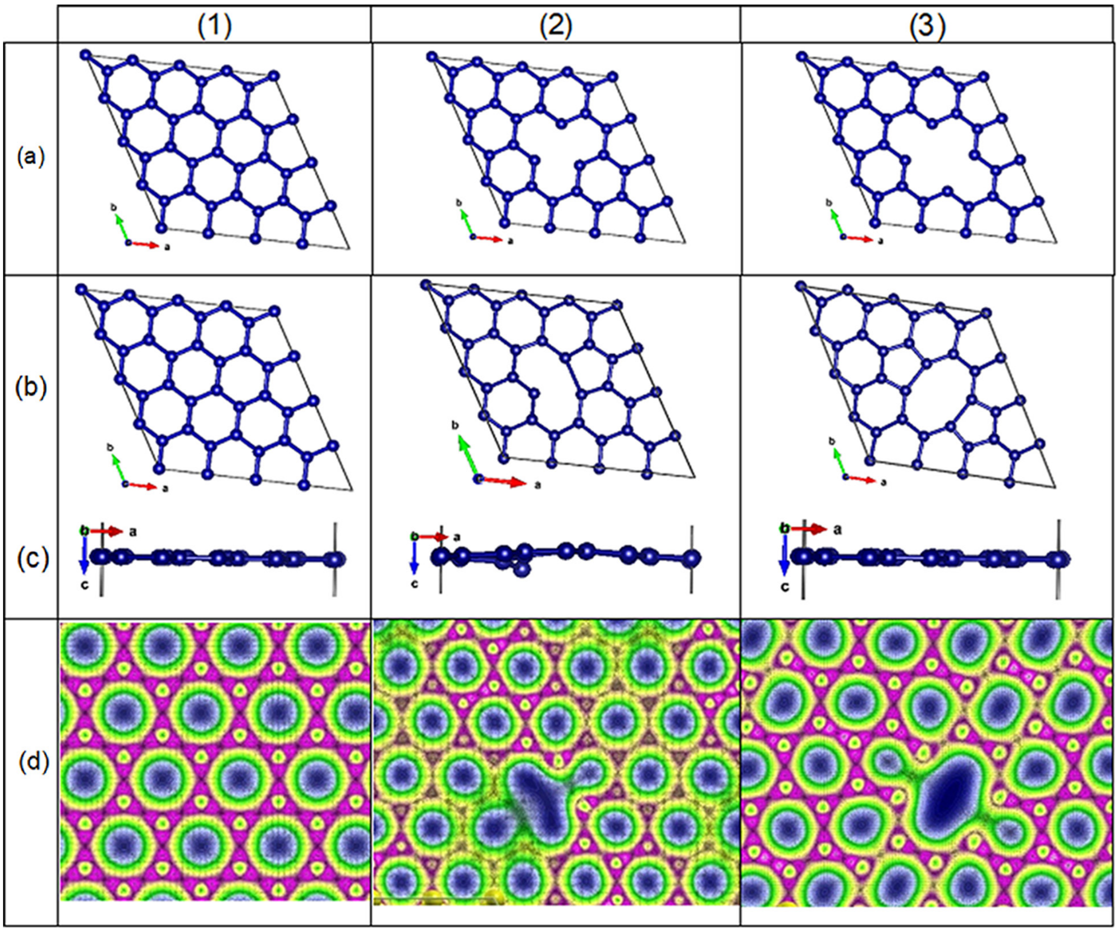

Figure 2. (a) Ideal geometry, (b) Reconstructed geometry (top view) and (c) Reconstructed geometry (side view), (d) Contour plot (1) PG, (2) SVG and (3) DVG.

when aligned in the zigzag direction, while a tetragon is formed when aligned in the armchair direction, due to the overlap of two pentagons. For the case of multi-vacancies with odd numbers of missing atoms, the formation of a bridging atom stabilizing the structure is observed in HRTEM [34].

The formation of a bridge rather than a reconstruction is preferred when a SVG merges with a DVG [35]. Indeed, in two distinct studies, one group imaged reconstructed TVG and the other group imaged TVG-bridge. They attributed this discrepancy to the different method used for defect creation. The former group used high velocity ions to bombard the graphene sheet, which is able to remove three adjust carbon atoms, however, the latter group used electron collision which is limited to sputtering a single carbon atom and can form double vacancies under continued irradiation.

Table 1. Characteristics of carbon vacancies in graphene.

Vacancy type	Formation energy (eV)		New bond length (Å)	
	This work	Literature [34]	This work	Literature [34]
Single	7.9	7.6-7.9	2.0	1.8-2
Double	3.9	3.1-4.4	1.8	1.6-1.8
Triple	3.9	3.9	1.9	1.8

The energy difference between the ideal and relaxed geometries of graphene with tri-vacancy defect has been reported in literature to be 228.6 kJ.mol^{-1} [36]. In our first attempt, we fully optimized a tri-vacancy in (4×4×1) supercell. As shown in Figure 3, reconstruction of tri-vacancy makes it more stable by the value of 157 kJ mol^{-1}. In reconstructed TVG, the under-coordinated carbon atoms stabilize themselves by interaction with each other and two five-member rings are formed. After reconstruction, all carbon atoms remain in graphene plane and the length of new bond between under-coordinated carbons is 1.9 Å, which is slightly stronger than that of new semi-bond in reconstructed SVG and slightly weaker than that of new semi-bond in reconstructed DVG (see Table 1). In comparison

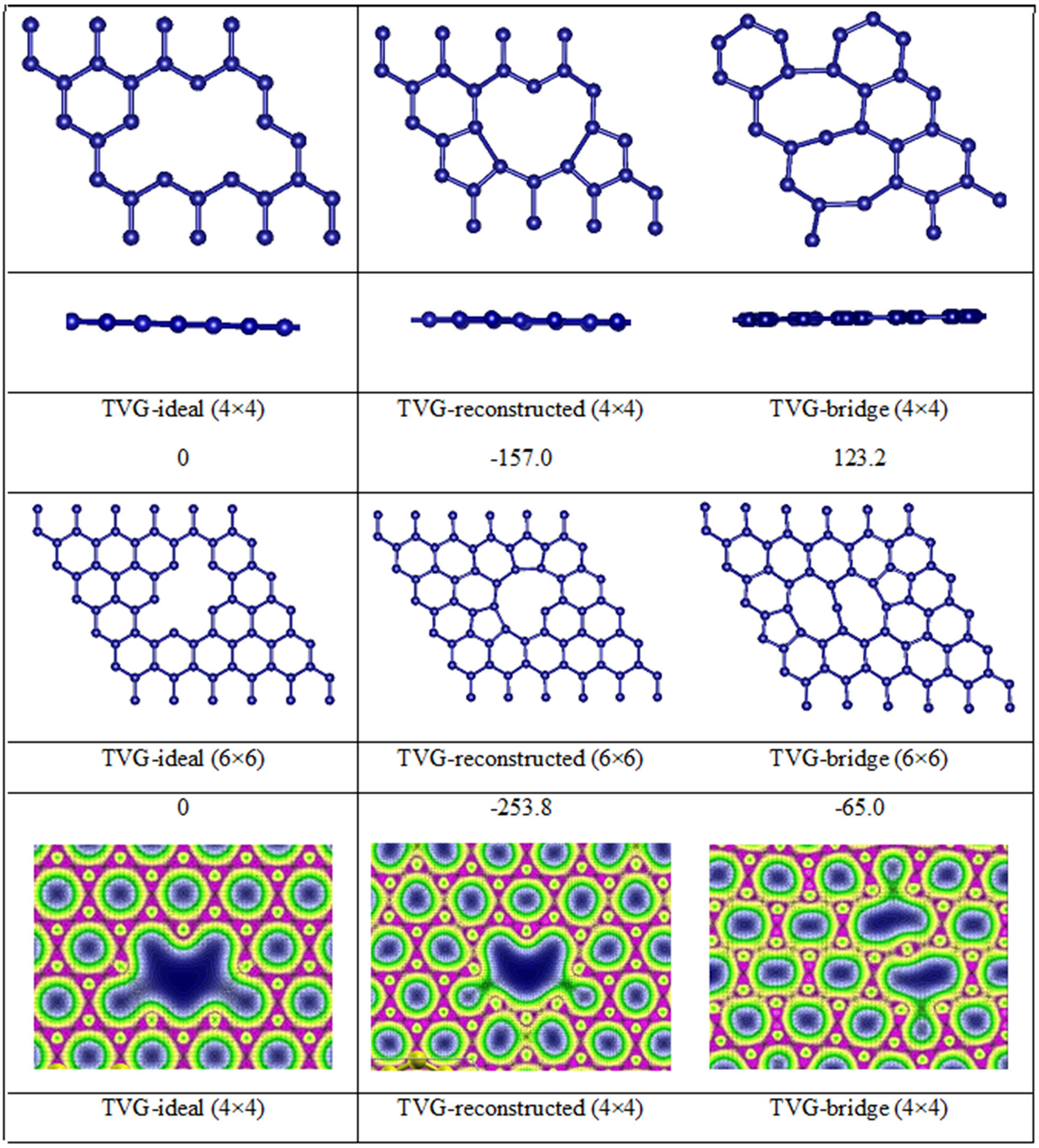

Figure 3. Geometry of ideal, reconstructed and bridge TVGs in (4×4) and (6×6) super-cells, relative energies in $kJ.mol^{-1}$ and corresponding contour plots.

with reconstruction TVG reported in literature, we achieved less stable geometry for TVG after optimization. Indeed, (4×4×1) supercell is not large enough to prevent the interaction of TVG with its image in a periodic boundary condition. Using (6×6×1) supercells, the reconstructed TVG is more stable by 253.8 kJ mol^{-1}, which is comparable with the previously reported value of 228.6 kJ mol^{-1}.

From literature, the DFT-calculated energy gain is 149.5 kJ mol^{-1} for a TVG-bridge, as compared to reconstructed TV G [34, 35]. In other words, the formation energy for reconstructed TVG has been reported to be 149.5 kJ mol^{-1} lower than that for TVG with a bridge. In a (4×4×1) and a (6×6×1) supercell, the reconstructed TVG is more stable than TVG-bridge by the value of 280.0 and 188.8 kJ mol^{-1}, respectively. Therefore, (4×4×1) supercell is not large enough to prevent the interaction of TVG with its image in periodic boundary condition and for accurate calculations, the larger supercell of TVG should be used.

Vacancy Formation Energy

There are different methods in literature for calculation of vacancy formation energy [34]. If the vacancy formation energy is defined as an average energy per vacant carbon atom in SVG (DVG), then the formation energy per vacant C atom (E_f) in each configuration can be calculated from Equation 2:

$$E_f = \frac{1}{n}(E_{v_n} - \frac{N - n}{N}E_{gra}) \tag{2}$$

Where, n is the number of vacant carbon atom in SVG, DVG or TVG, is the total energy of the SVG, DVG or TVG, N is the number of carbon atoms in supercell and Egra is the total energy of defect free graphene supercell with the same size.

As shown in Table 1, we found that the formation energy of single vacancy is 7.9 eV in agreement with experimental value of 7.0 ± 0.5 eV and other theoretical values ranging from 7.6 to 7.9 eV. The formation energy for double and triple vacancy both were calculated to be 3.9 eV, which is in agreement with the literature. Therefore, the structures are in their relaxed states and the force and energy restrictions used in our calculations are in reasonable ranges. Moreover, double vacancy should be easy to form from existing mono vacancies and is stable at room temperature.

Ethylene Adsorption on PG, SVG and DVG

Van der Waals interaction is a weak long-range interaction and chemisorption is a strong short-range interaction. Therefore, the initial distance between ethylene and GS should be selected in a such proper range that includes both interactions by considering the point that the whole geometry is the most stable geometry relative to other geometries with the same chemical structure. In order to determine the nature of ethylene adsorption (physisorption or chemisorption) on GS, several full optimization calculations were done by putting ethylene at different initial distance and various orientation with respect to the surface of GS. In some cases, ethylene, GS or both deformed due to adsorption. Therefore, both adsorption and deformation energies were calculated to verify reasonability of structural changes due to ethylene adsorption. The ethylene adsorption energy on each GS was calculated from equation 1 as mentioned former and as follows:

$$E_{ads}(Ethylene) = E(Eth / GS) - E(Eth) - E(GS)$$

In which, $E_{ads\ (Ethylene)}$ is the ethylene adsorption energy, *E(Eth/GS)* is the energy of ethylene adsorbed GS, *E(Eth)* and *E(GS)* are the ethylene and GS energies, respectively.

Furthermore, the total deformation energy of ethylene and GS due to adsorption (E_{def}) was calculated from below equations:

$$E_{def} = E_{def}(GS) + E_{def}(Eth) \tag{3}$$

$$E_{def}(GS) = E_{Eth}(GS) + E(GS) \tag{4}$$

$$E_{def}(Eth) = E_{GS}(Eth) - E(Eth) \tag{5}$$

In which, $E_{def}(GS)$ is the deformation energy of GS, $E_{Eth}(GS)$ is the energy of deformed GS due to ethylene adsorption and *E(GS)* is the energy of isolated non-deformed GS. Similarly, $E_{def}(Eth)$ is the deformation energy of ethylene, $E_{GS}(Eth)$ is the energy of deformed ethylene due to adsorption on GS, and *E(Eth)* is the energy of isolated non-deformed ethylene. All deformation energies are always positive.

By subtracting the total deformation energy (E_{def}) from ethylene adsorption energy ($E_{ads}(Ethylene)$), a new type of adsorption energy is defined in which, the geometrical changes due to adsorption have no contribution.

$$E'_{ads}(Ethylene) = E(Eth - GS) - E_{Eth}(GS) - E_{GS}(Eth) \tag{6}$$

Finally, from all above equations it can be demonstrated that:

$$E_{ads}(Ethylene) = E'_{ads}(Ethylene) + E_{def}(Eth) \tag{7}$$

In this study, all the adsorption energies were calculated using Equation 1, in which the structural change due to adsorption play a role in the adsorption energy.

The result of these calculations for ethylene adsorption on PG, SVG, DVG-Hole and DVG-Bridge have been collected in Table 2 to Table 5. From Table 2, the ethylene adsorption on PG at initial distance of 1.5 and 1.7 Å is endothermic by the value of 31.9 kJ mol^{-1}. At initial distance of 1.9 Å and more, the adsorption energy becomes exothermic by the value of 99.0 kJ mol^{-1}. Therefore, the adsorption of ethylene on PG is a physisorption dominated by vdW interaction. The proper initial distance for accurate calculation of adsorption energy on PG is 1.9 Å or a bit more. Ethylene adsorption on PG is a physisorption.

From Table 3, ethylene adsorption on SVG is a chemisorption. The proper initial distance for accurate calculation of adsorption energy on SVG is less than 2.1 Å. Ethylene adsorption on DVG-bridge is a chemisorption, ethylene is able to heal the DVG and the product will be partially hydrogenated Stone-Wale defected graphene. However, ethylene more prefers to be chemisorbed on the DVG-bridge rather than to heal it. Finally, from both Table 4 and Table 5, ethylene is able to heal DVG and depending on initial orientation of ethylene with respect to DVG (on hole or on bridge), defect free graphene or graphene with a Stone-Wales defect could be produced after dehydrogenation. A Stone-Wales defect (SW) is a point defect that involves the change of connectivity of two carbon atoms, leading to their rotation by 90° with respect to the midpoint of their bond. This rearrangement creates a structure with less resonance stabilization among the sp^2 atoms involved and higher strain energy in the local structure. As a result, the defect creates a region with greater chemical reactivity, including acting as a nucleophile and creating a preferred site for binding to hydrogen atoms. Regardless of being the lowest-energy defect in graphene and other sp2-hybridized carbon nanostructures, SW needs about 5 eV to appear in graphene [37].

DVG-Hole prefers to be healed by ethylene as the ethylene adsorption is the most exothermic one in healed DVG-Hole. On the other hand, ethylene prefers to be chemisorbed on DVG-Bridge as the graphene with SW defect is less stable than ethylene chemisorbed DVG-Bridge by 41.5 kJ mol^{-1}. Furthermore, ethylene chemisorption on the bridge position in DVG is more exothermic than the hole position by 76.1 $kJ.mol^{-1}$ because lower distance between two remaining dangling bond after ethylene adsorption on bridge position makes it possible for two under-coordinated carbon atoms to interact with each other and stabilize themselves. This exothermic energy is less than half of the DVG reconstruction energy (-189 $kJ.mol^{-1}$). Indeed,

Table 2. Geometry, deformation and adsorption energy of ethylene/PG system.

Initial Distance (Å)	Deformation Energy ($kJ.mol^{-1}$)	Final Distance (Å)	Ethylene Adsorption Energy ($kJ.mol^{-1}$)	Final Geometry
1.5	370.8	1.6	31.9	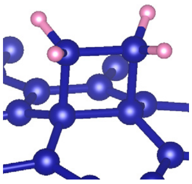
1.7	370.8	1.6	31.9	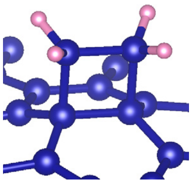
1.9	0.0	3.4	-99.0	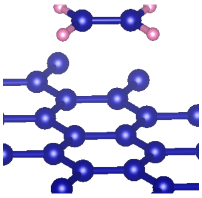
2.1	0.0	3.4	-99.0	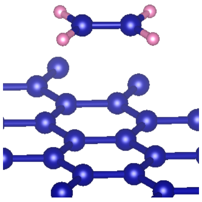

Table 3. Geometry, deformation and adsorption energy of ethylene/SVG system.

Initial Distance (Å)	Deformation Energy (kJ.mol^{-1})	Final Distance (Å)	Ethylene Adsorption Energy (kJ.mol^{-1})	Final Geometry
1.5	338.7	1.5	-423.8	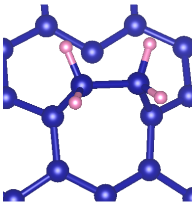
1.7	338.7	1.5	-423.8	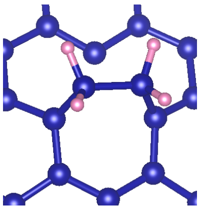
1.9	338.7	1.5	-423.8	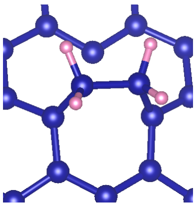
2.1	338.7	1.5	-423.8	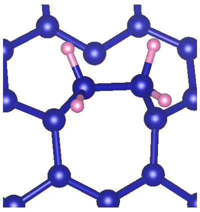
3.2	0.0	3.2	-93.1	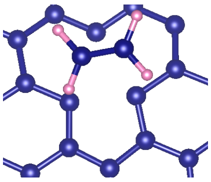

after ethylene chemisorption on DVG-Bridge, the distance between two remaining under-coordinated carbon atoms was 2.0 Å, which is slightly higher than 1.9 Å in reconstructed DVG.

It should be noted that, since complete healing of DVG occurs at very low initial ethylene distance, ethylene should pass a barrier at critical distance to heal the DVG (see Figure 4). Indeed, as ethylene is brought closer to the vacancy site, there may be a barrier at a critical height. At initial distance larger than this height, ethylene either may go away from the surface (in the case of PG) or be trapped at lower height (in the case of SVG). However, as soon as ethylene gets closer than the critical height, it is attracted toward the defect site by chemical interaction forces and moves even closer to be adsorbed as a molecule on vacancy and in the case of DVG finally be a part of graphene plane [38]. In other words, the initial distance between ethylene and GBMs can be divided into three regions by two critical heights: physisorption, chemisorption and healing. Ethylene interacts with PG, SVG and DVG at physisorption, chemisorption and healing region, respectively. The critical height of ethylene to be chemisorbed on SVG is higher than that of DVG-Bridge and this height for DVG-hole is the least. Therefore, SVG is more sensitive to its environment than DVG.

Second Ethylene Adsorption on SVG and DVG

The interaction of second ethylene with the first

Table 4. Geometry, deformation and adsorption energy of ethylene/DVG-Hole system.

Initial Distance (Å)	Deformation Energy (kJ.mol^{-1})	Final Distance (Å)	Adsorption Energy (kJ. mol^{-1})	Final Geometry
-	-	-	-538.8	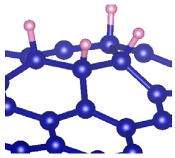
1.4	1026.6	1.51-1.57	-367.5	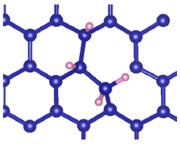
1.5	435.3	1.57	-199.8	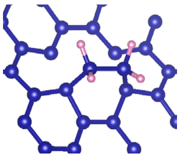
1.7	435.3	1.57	-199.8	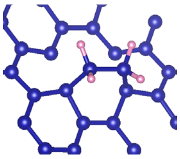
1.9	0.0	3.2	-93.8	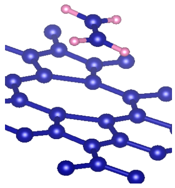
2.1	0.0	3.2	-93.8	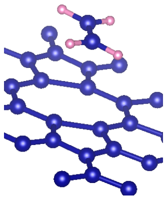

ethylene chemisorbed on the single vacancy of graphene and with healed double vacancy on graphene was studied. After the first ethylene chemisorption on SVG, one carbon remains under-coordinated, so we tried to evaluate if the reaction of a second ethylene is possible via this extremely active species. First, we tried to examine the accessibility of this under-coordinated carbon for second ethylene (Figure 5). Then, we examined the interaction of second ethylene with the first ethylene adsorbed on SVG by scanning the distance between two carbon atoms of two ethylene molecules. At large distance, the second ethylene physisorption is exothermic by the value of 8.9 kJ mol^{-1} and chemical bonding is observed neither between two ethylene nor between second ethylene and under-coordinated carbon of SVG. As the distance between two ethylene molecules reduces, the interaction energy increases and at distances lower than 2.9 Å, the interaction becomes endothermic (Figure 6). Due to the large hindrance of the first chemisorbed ethylene and small size of the under-coordinated carbon atom, this atom is not accessible for the second ethylene adsorption. Therefore, the second ethylene neither has suitable interaction with the active carbon atom at the edge of SVG nor with the first adsorbed ethylene.

Furthermore, ethylene adsorption on DVG results in healing of DVG with ethylene and partially hydrogenated PG is produced. The interaction of second ethylene with this partially hydrogenated graphene was also studied (Figure 7). It was found that the second

Table 5. Geometry, deformation and adsorption energy of ethylene/DVG-Bridge system.

Initial Distance (Å)	Deformation Energy ($kJ.mol^{-1}$)	Final Distance (Å)	Ethylene Adsorption Energy ($kJ.mol^{-1}$)	Final Geometry
1.51	-	1.51	-232.9	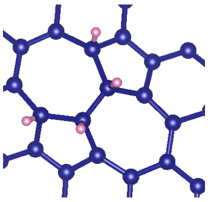
1.5	499.4	1.51	-275.0	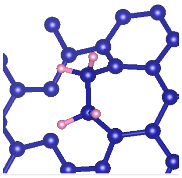
1.7	499.4	1.51	-275.0	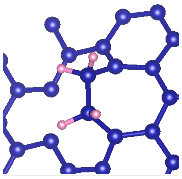
1.9	499.4	1.51	-275.0	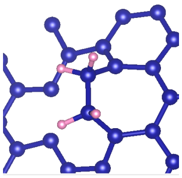
2.1	0	3.3	-90.8	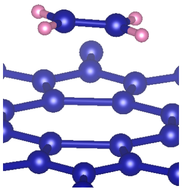

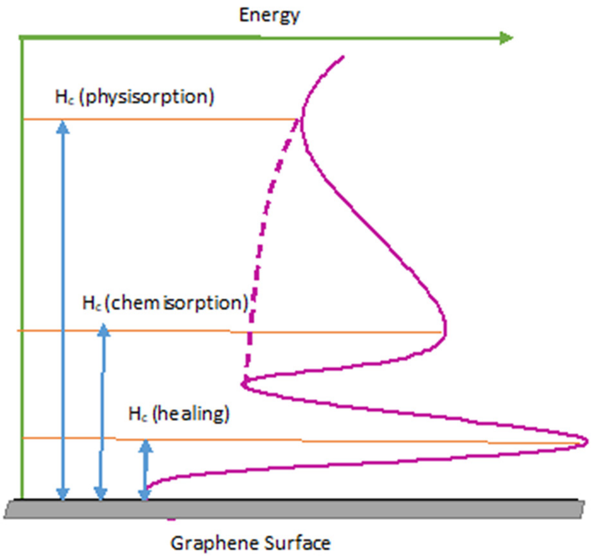

Figure 4. Schematic minimum energy path for interaction of ethylene with DVG.

ethylene is hydrogenated on partially hydrogenated graphene and ethane is produced. The hydrogenation of ethylene on partially hydrogenated graphene is predicted to be exothermic by 169.2 kJ mol^{-1}.

Ethylene Adsorption on TVG and TVGB

The ethylene interaction with reconstructed TVG was

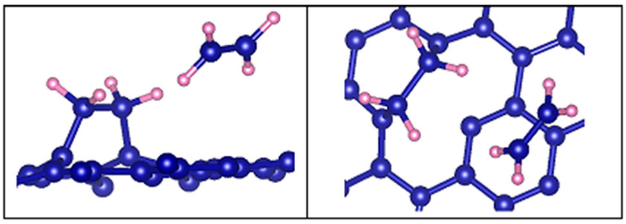

Figure 5. Schematic representation of accessibility of the under-coordinated carbon for the adsorption of the second ethylene in SVG.

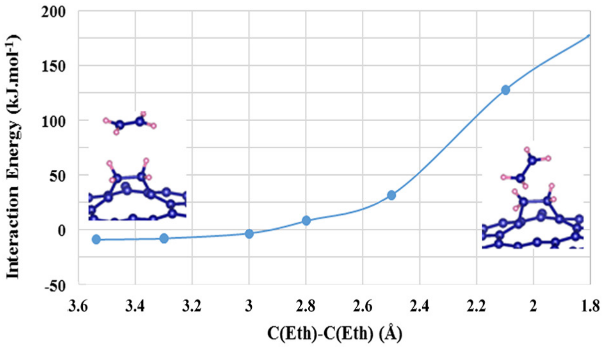

Figure 6. Minimum energy path for the interaction of the second ethylene on ethylene adsorbed-SVG. Atomic configurations correspond to 3.6 and 1.8 Å of reaction coordinate.

investigated by considering three different initial orientations of ethylene on this defective graphene, and the results have been collected in Table 6. In geometry 1, the carbene and one carbon of five-member rings; in geometry 2, two carbon atoms of two five-member rings and in geometry 3, two carbon atoms of one five-member ring were considered as potential active sites. Geometry 1 is more energetically favourable due to the existence of no under-coordinated carbon in the final geometry. In geometry 3, the reactive carbene abstracts one hydrogen of ethylene and the dehydrogenation reaction occurs. By considering the number of remaining under-coordinated carbon atoms after ethylene interaction with reconstructed TVG, the difference between adsorption energies in Table 6 can be explained. In geometry 1, there are three under-coordinated carbon atoms, and two of them are stabilized by interacting with each other. In geometry 2, there are three under-coordinated carbon atoms with no interaction. Finally, in geometry 3, two under-coordinated carbon atoms interact with each other. Therefore, geometry 3 is the most energetically favourable geometry for ethylene interaction with reconstructed TVG.

The interaction of ethylene with TVGB was investigated by considering two different initial orientations of ethylene on a bridge and two carbon atoms of one five-member ring. From Table 6, ethylene prefers to be adsorbed on the under-coordinated atoms in the edge of the five-member ring. In geometry 1, the length of one involved bond in the bridge increases from 1.5 to 1.7 Å. Therefore, the carbon atom at the bridge's center becomes more reactive after ethylene adsorption.

CONCLUSIONS

For many applications, it is important to understand how graphene and its derivatives interact with other molecules in its vicinity. Considering metal comperable graphene activity in selective acetylene hydrogenation in the presence of large excess ethylene, theoretical study of the interaction of ethylene with intrinsic defects of graphene is intresting. It is common to use adsorption energy to differentiate between physical and chemical adsorption, however; it is not a reliable

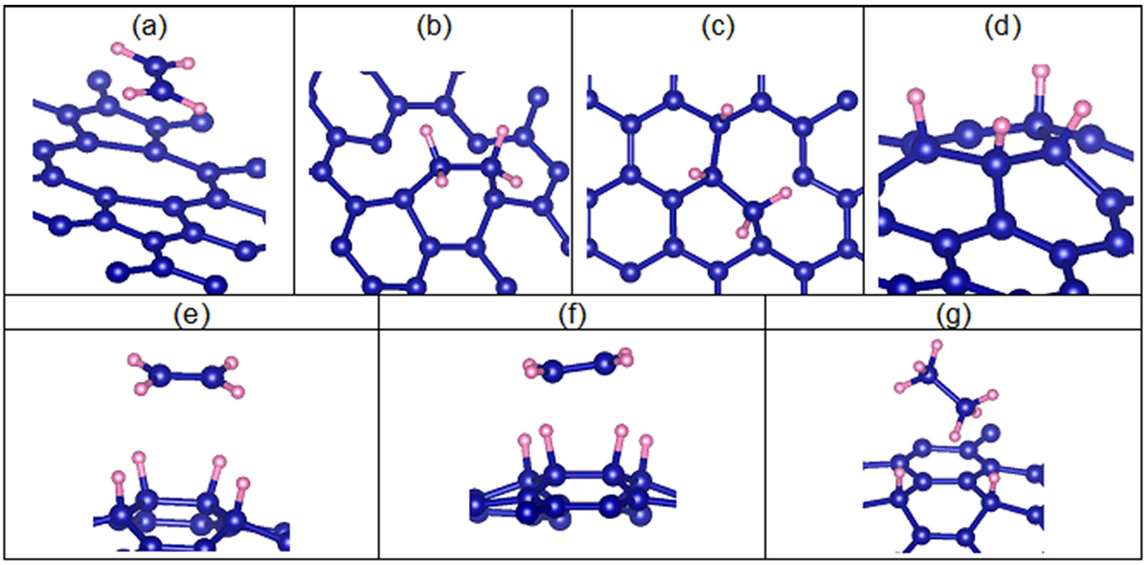

Figure 7. Schematic representation of healing of DVG-Hole by ethylene and interaction of the second ethylene with healed DVG, giving ethane.

Table 6. Ethylene adsorption on TVG and TVGB (all energies are in kJ mol^{-1}).

<table>
<tr><th colspan="4">Three geometries for ethylene adsorption on TVG</th></tr>
<tr><td>Top view</td><td>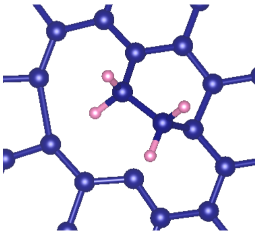</td><td>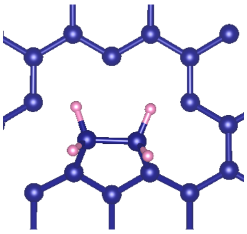</td><td>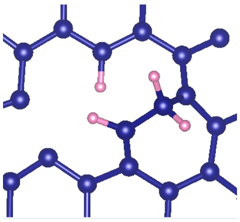</td></tr>
<tr><td>Side view</td><td>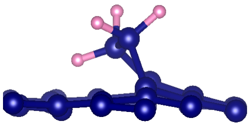</td><td>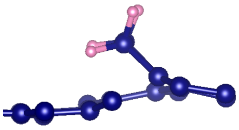</td><td>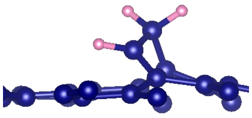</td></tr>
<tr><td>Geometry</td><td>(1)</td><td>(2)</td><td>(3)</td></tr>
<tr><td>Adsorption energy</td><td>-456.9</td><td>-257.6</td><td>-603.1</td></tr>
<tr><th colspan="4">Two geometries for ethylene adsorption on TVGB</th></tr>
<tr><td>Top view</td><td colspan="2">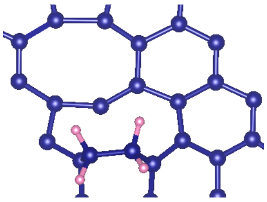</td><td>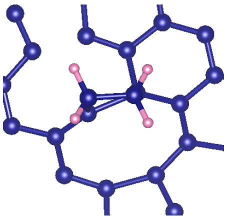</td></tr>
<tr><td>Side view</td><td colspan="2">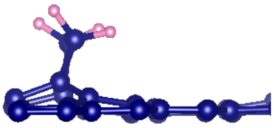</td><td>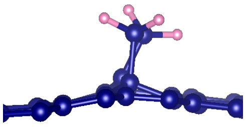</td></tr>
<tr><td>Geometry</td><td colspan="2">(1)</td><td>(2)</td></tr>
<tr><td>Adsorption energy</td><td colspan="2">-324.3</td><td>-288.0</td></tr>
</table>

criterion. There is a critical distance from the graphene surface, where the nature of adsorption of adsorbate molecules changes from physisorption to the possible chemisorption depending on the energetical costly distortion induced in adsorbate molecule. In the case of ethylene adsorption on the graphene structures studied here, the critical distance follows this order SVG< DVG< PG. However, in the range of vdW domination and comparison with PG, ethylene interacts more with SVG due to the presence of a dangling bond and less with DVG due to the presence of a hole. Therefore, SVG is more sensitive to its environment than DVG. Ethylene is able to heal DVG and depending on initial orientation of ethylene with respect to DVG (on hole or on bridge), defect free graphene or graphene with a Stone-Wales defect could be produced after dehydrogenation. In reconstructed TVG, the under-coordinated carbon atoms stabilize themselves by interaction with each other and two five-member ring are formed. After reconstruction, all carbon atoms remain in graphene plane and the length of new bond between under-coordinated carbons is 1.9 Å, which is slightly longer than that of new bond in reconstructed SVG and slightly smaller than that of new bond in reconstructed DVG. Finally, the general view presented in this study on ethylene interaction with intrinsic defects of graphene and previous studies in literature may be helpful in paving the way for more comprehensive mechanistic studies to shed light on the exact graphene active sites.

ACKNOWLEDGEMENTS

P. Alamdari, F. Sharif, and S. Mazinani are grateful for funding from the Iranian Ministry of Science, Research and Technology (MSRT). PA thanks ASIC-UPV for use of computational facilities.

CONFLICTS OF INTEREST

The author declares that they have no conflicts of interest.

REFERENCES

1. Novoselov KS, Geim AK, Morozov SV, Jiang D-E, Zhang Y, Dubonos SV, Grigorieva IV, Firsov AA (2004) Electric field effect in atomically thin carbon films. Science 306: 666-669
2. Navalon S, Dhakshinamoorthy A, Alvaro M, Garcia H (2014) Carbocatalysis by graphene-based materials. Chem Rev 114: 6179-6212
3. Fan X, Zhang G, Zhang F (2015) Multiple roles of graphene in heterogeneous catalysis. Chem Soc Rev 44: 3023-3035
4. Antonietti M, Navalón S, Dhakshinamoorthy A, Álvaro M, García H (2018) Carbocatalysis: Analyzing the sources of organic transformations. In: Carbon-based metal-free catalysts: Design and applications 1, 285-311
5. Nag A, Mitra A, Mukhopadhyay SC (2018) Graphene and its sensor-based applications: A review. Sens Actuator A Phys 270: 177-194
6. Liu G, Jin W, Xu N (2015) Graphene-based membranes. Chem Soc Rev 44: 5016-5030
7. Gao Y, Neal L, Ding D, Wu W, Baroi C, Gaffney AM, Li F (2019) Recent advances in intensified ethylene production-A review. ACS Catal 9: 8592-8621
8. Primo A, Neatu F, Florea M, Parvulescu V, Garcia H (2014) Graphenes in the absence of metals as carbocatalysts for selective acetylene hydrogenation and alkene hydrogenation. Nat commun 5: 5291
9. Perhun TI, Bychko IB, Trypolsky AI, Strizhak PE (2013) Catalytic properties of graphene material in the hydrogenation of ethylene. Theor Exp Chem 48: 367-370
10. Abakumov AA, Bychko IB, Nikolenko AS, Strizhak PE (2018) Catalytic activity of n-doped reduced graphene oxide in the hydrogenation of ethylene and acetylene. Theor Exp Chem 54: 218-224
11. Zhang X, Kumari G, Heo J, Jain PK (2018) In situ formation of catalytically active graphene in ethylene photo-epoxidation. Nat Commun 9: 3056
12. Chang J, Zhang Y, Yao Y, Liu X, Hildebrandt D (2022) Reduced graphene oxide supported cobalt catalysts for ethylene hydroformylation: Modified cobalt-support interaction by rhodium. Fuel 324: 124479
13. Liu X, Yang Y, Chu M, Duan T, Meng C, Han Y (2016) Defect stabilized gold atoms on graphene as potential catalysts for ethylene epoxidation: A first-principles investigation. Catal Sci Technol 6: 1632-1641
14. Navalon S, Dhakshinamoorthy A, Alvaro M, Antonietti M, García H (2017) Active sites on graphene-based materials as metal-free catalysts. Chem Soc Rev
15. Stephan DW, Erker G (2010) Frustrated Lewis pairs: Metal-free hydrogen activation and more. Angew Chem Int Ed 49: 46-76
16. Sastre G, Forneli A, Almasan V, Parvulescu VI, Garcia H (2017) Isotopic h/d exchange on graphenes. A combined experimental and theoretical study. Appl Catal 547: 52-59
17. Lee JS, Ko YS (2014) Synthesis of petaloid graphene/polyethylene composite nanosheet produced by ethylene polymerization with metallocene catalyst adsorbed on multilayer graphene. Catal Today 232: 82-88
18. Nia AS, Binder WH (2017) Graphene as initiator/catalyst in polymerization chemistry. Prog Polym Sci 67: 48-76
19. Zhang H-X, Ko E-B, Park J-H, Moon Y-K, Zhang X-Q, Yoon K-B (2016) Fabrication of polyethylene/graphene nanocomposites through in situ polymerization with a spherical graphene/$MgCl_2$-supported Ziegler-Natta catalyst. Compos Sci Technol 136: 61-66
20. Kheradmand A, Ramazani Sa A, Khorasheh F, Baghalha M, Bahrami H (2015) Effects of nano graphene oxide as support on the product properties and performance of Ziegler–Natta catalyst in production of UHMWPE. Polym Adv Technol

26: 315-321

21. Zhang H, Park J-H, Moon Y-K, Ko E-B, Lee D-H, Hu Y, Zhang X, Yoon K-B (2017) Preparation of graphene/$MgCl_2$-supported Ti-based Ziegler-Natta catalysts by the coagglomeration method and their application in ethylene polymerization. Chinese J Catal 38: 131-137
22. Chmutin I, Novokshonova L, Brevnov P, Yukhayeva G, Ryvkina N (2017) Electrical properties of UHMWPE/graphite nanoplates composites obtained by in-situ polymerization method. Polyolefins J 4: 1-12
23. Abdolahzadeh T, Morshedian J, Ahmadi S (2022) Preparation and characterization of nano WO_3/Bi_2O_3/GO and $BaSo_4$/GO dispersed HDPE composites for X-ray shielding application. Polyolefins J 9: 73-83
24. Shehzad F, Daud M, Al-Harthi MA (2016) Synthesis, characterization and crystallization kinetics of nanocomposites prepared by in situ polymerization of ethylene and graphene. J Therm Anal 123: 1501-1511
25. Li K, Li N, Yan N, Wang T, Zhang Y, Song Q, Li H (2020) Adsorption of small hydrocarbons on pristine, n-doped and vacancy graphene by DFT study. Appl Surf Sci 515: 146028
26. Wang C, Xiao B, Ding Y-H (2013) Theoretical investigation on the healing mechanism of divacancy defect in graphene growth by reaction with ethylene and acetylene. New J Chem 37: 640-645
27. Kokalj A (2022) Corrosion inhibitors: Physisorbed or chemisorbed? Corros Sci 196: 109939
28. Giannozzi P, Baroni S, Bonini N, Calandra M, Car R, Cavazzoni C, Ceresoli D, Chiarotti GL, Cococcioni M, Dabo I (2009) Quantum espresso: A modular and open-source software project for quantum simulations of materials. J Phys Condens 21: 395502
29. Giannozzi P, Andreussi O, Brumme T, Bunau O, Nardelli MB, Calandra M, Car R, Cavazzoni C, Ceresoli D, Cococcioni M (2017) Advanced capabilities for materials modelling with quantum espresso. J Phys Condens 29: 465901
30. Monkhorst HJ, Pack JD (1976) Special points for brillouin-zone integrations. Phys Rev B 13: 5188
31. Perdew JP, Burke K, Ernzerhof M (1996) Generalized gradient approximation made simple. Phys Rev lett 77: 3865
32. Perdew JP, Ruzsinszky A, Csonka GI, Vydrov OA, Scuseria GE, Constantin LA, Zhou X, Burke K (2008) Restoring the density-gradient expansion for exchange in solids and surfaces. Phys Rev lett 100: 136406
33. Grimme S, Antony J, Ehrlich S, Krieg H (2010) A consistent and accurate ab initio parametrization of density functional dispersion correction (DFT-d) for the 94 elements H-Pu. Chem Phys 132: 154104
34. Skowron ST, Lebedeva IV, Popov AM, Bichoutskaia E (2015) Energetics of atomic scale structure changes in graphene. Chem Soc Rev 44: 3143-3176
35. Robertson AW, Lee G-D, He K, Yoon E, Kirkland AI, Warner JH (2014) The role of the bridging atom in stabilizing odd numbered graphene vacancies. Nano Lett 14: 3972-3980
36. Yamashita K, Saito M, Oda T (2006) Atomic geometry and stability of mono-, di-, and trivacancies in graphene. Jpn J Appl Phys 45: 6534
37. Kotakoski J, Meyer J, Kurasch S, Santos-Cottin D, Kaiser U, Krasheninnikov A (2011) Stone-wales-type transformations in carbon nanostructures driven by electron irradiation. Phys Rev B 83: 245420
38. GüRel HH, Ozçelik VO, Ciraci S (2014) Dissociative adsorption of molecules on graphene and silicene. Phys Chem C 118: 27574-27582